

Thermodynamic Hydricities of Biomimetic Organic Hydride Donors

Stefan Ilic, Usha Pandey Kadel, Yasemin Basdogan, John A. Keith, and Ksenija D. Glusac

J. Am. Chem. Soc., **Just Accepted Manuscript** • DOI: 10.1021/jacs.7b13526 • Publication Date (Web): 16 Mar 2018

Downloaded from <http://pubs.acs.org> on March 17, 2018

Just Accepted

“Just Accepted” manuscripts have been peer-reviewed and accepted for publication. They are posted online prior to technical editing, formatting for publication and author proofing. The American Chemical Society provides “Just Accepted” as a service to the research community to expedite the dissemination of scientific material as soon as possible after acceptance. “Just Accepted” manuscripts appear in full in PDF format accompanied by an HTML abstract. “Just Accepted” manuscripts have been fully peer reviewed, but should not be considered the official version of record. They are citable by the Digital Object Identifier (DOI®). “Just Accepted” is an optional service offered to authors. Therefore, the “Just Accepted” Web site may not include all articles that will be published in the journal. After a manuscript is technically edited and formatted, it will be removed from the “Just Accepted” Web site and published as an ASAP article. Note that technical editing may introduce minor changes to the manuscript text and/or graphics which could affect content, and all legal disclaimers and ethical guidelines that apply to the journal pertain. ACS cannot be held responsible for errors or consequences arising from the use of information contained in these “Just Accepted” manuscripts.



Thermodynamic Hydricities of Biomimetic Organic Hydride Donors

Stefan Ilic[‡], Usha Pandey Kadel[§], Yasemin Basdogan^b, John A. Keith^b, Ksenija D. Glusac^{‡*}

[‡]Department of Chemistry, University of Illinois at Chicago, Chicago, IL 60607, United States

[‡]Chemical Sciences and Engineering Division, Argonne National Laboratory, Lemont, IL 60439, United States

[§]Department of Chemistry, Center for Photochemical Sciences, Bowling Green State University, Bowling Green, OH 43403, United States

^bDepartment of Chemical and Petroleum Engineering, University of Pittsburgh, Pittsburgh, PA 15260, United States

ABSTRACT: Thermodynamic hydricities (ΔG_{H^-}) in acetonitrile and dimethyl sulfoxide have been calculated and experimentally measured for several metal-free hydride donors: NADH analogs (BNAH, CN-BNAH, Me-MNAH, HEH), methylene tetrahydromethanopterin analogs (BIMH, CAFH), acridine derivatives (Ph-AcrH, Me₂N-AcrH, T-AcrH, 4OH, 2OH, 3NH) and a triarylmethane derivative (6OH). The calculated hydricity values, obtained using density functional theory, showed a reasonably good match (within 3 kcal/mol) with the experimental values, obtained using “potential-pKa” and “hydride-transfer” methods. The hydride donor abilities of model compounds were in the 48.7 – 85.8 kcal/mol (acetonitrile) and 46.9 – 84.1 kcal/mol (DMSO) range, making them comparable to previously studied first-row transition metal hydride complexes. To evaluate the relevance of entropic contribution to the overall hydricity, Gibbs free energy differences (ΔG_{H^-}) obtained in this work were compared with the enthalpy (ΔH_{H^-}) values obtained by others. The results indicate that, even though ΔH_{H^-} values exhibit the same trends as ΔG_{H^-} , the differences between room-temperature ΔG_{H^-} and ΔH_{H^-} values range from 3 to 9 kcal/mol. This study also reports a new metal-free hydride donor, namely an acridine-based compound 3NH, whose hydricity exceeds that of NaBH₄. Collectively, this work gives a perspective of use metal-free hydride catalysts in fuel-forming and other reduction processes.

INTRODUCTION

Enzymatic redox reactions often rely on organic cofactors, such as reduced nicotinic adenine dinucleotide (NADH) and flavin adenine dinucleotide (FADH₂), to perform hydride transfer reactions to substrates such as carbonyl compounds,¹ carbon dioxide,² flavins (imines),³ and compounds containing activated C=C bonds.⁴⁻⁵ The synthetic analogs of these biological “H₂-equivalents” have found applications in chemical laboratories, particularly when asymmetric transformations are desired. In the presence of a chiral co-catalyst, NADH-analogs serve as regio- and enantioselective reagents for the reduction of imines to amines,⁶⁻⁸ carbonyl compounds to alcohols,⁸⁻¹⁰ as well as compounds with C=C bonds to the corresponding saturated analogs.^{8, 11-12} NADH analogs have also been applied to the fuel forming reactions. Specifically, a simple pyridinium ion has been investigated as facilitating the electrocatalytic and photoelectrocatalytic reduction of CO₂ to methanol.¹³⁻¹⁶ While the experimental work was not reproduced by others¹⁶ and the mechanism of catalysis still remains unclear, the computational work indicates that the CO₂ reduction may occur by a hydride transfer from dihydropyridine, a close relative of NADH.¹⁷⁻²¹ More recently, other nitrogen-containing organic compounds (imidazoles,²²⁻²³ pyridazine,²⁴ pyridoxine,²⁵ mercaptopteridine,²⁶⁻²⁸ dihydrophenanthridine²⁹ and dihydroacridine²⁹) have also been shown to perform CO₂ reduction reactions. Furthermore, NADH analog-based ligands coordinated with redox-

1
2
3 active transition metal (Ru,³⁰ Ir³¹) or other metal ions (Al³²) were shown to perform the photocatalytic or
4 electrocatalytic reduction of CO₂ or water.
5
6

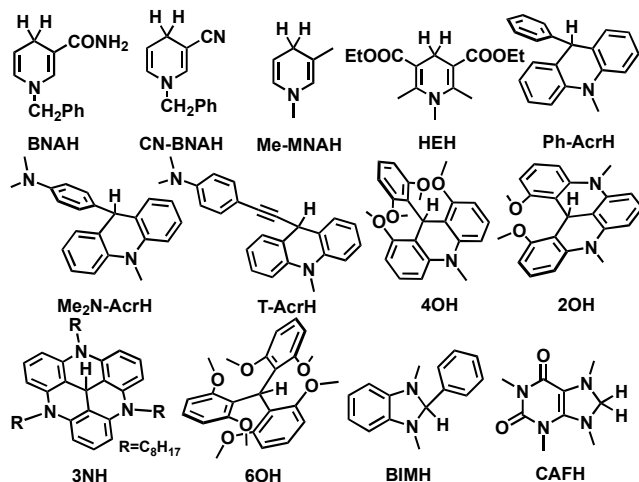
7 Thermodynamic hydricity (ΔG_{H^-}) is a useful parameter that is often used to evaluate the hydride donating
8 ability of a molecule. It is defined as the Gibbs free energy for a hydride-ion release from the compound, with
9 lower values of ΔG_{H^-} indicating better hydride donors:
10



14 This thermodynamic parameter provides useful information for the potential application of hydrides in
15 synthetic reductions of C=C, C=N and C=O bonds as well as in fuel-forming reductions of protons and CO₂. For
16 this reason, the hydricities of a large number of metal-based hydrides have been extensively studied using
17 computational and experimental methods for different solvents.³³⁻³⁹ Although ΔG_{H^-} values exhibit strong solvent
18 effects,⁴⁰⁻⁴² the majority of reported hydricities were obtained in acetonitrile. These hydricities were found to
19 vary in a wide 25 – 120 kcal/mol range. Relevant to fuel-forming reactions in acetonitrile, hydrides with ΔG_{H^-}
20 below 76 kcal/mol are thermodynamically capable of proton reduction,⁴³⁻⁴⁴ whereas ΔG_{H^-} below 44 kcal/mol is
21 needed for the reduction of CO₂ to formate.⁴⁵ The hydricity studies on metal-based models have shown several
22 structural factors that influence the ΔG_{H^-} values of metal hydrides: (i) the type of the metal used significantly
23 alters the hydricities of complexes. Within the same row of the periodic table, metals with lower atomic number
24 give rise to metal complexes with greater hydride donor ability.⁴⁶ Within the same group, metals in second and
25 third rows are generally better hydride donors than the first-row analogues;^{33, 44, 47-48} (ii) the structural and
26 electronic properties of the ligand can also tune the hydricities. For example, the decrease in the ligand bite angle
27 contributes to the lowering of ΔG_{H^-} values.⁴⁸⁻⁵⁰ Furthermore, the presence of electron-donating substituents on
28 the ligand decreases the hydricities of metal complexes;^{44, 51-53} (iii) the overall charge of the metal complex also
29 affects the hydricities, with anionic complexes being stronger hydride donors than the corresponding neutral
30 analogs;⁵⁴⁻⁵⁶ (iv) solvent drastically affects hydricities, where more polar solvents (such as water) lower ΔG_{H^-}
31 values.^{37, 40, 57-61} It is interesting to note that the hydricity values in different solvents do not scale linearly, making
32 it possible for a certain reaction to be thermodynamically downhill in one solvent, while uphill in another.⁵⁷
33
34
35
36
37
38
39
40

41 A systematic analysis of over 150 reported hydricity values for metal-based hydride donors has enabled the
42 discovery of many elegant catalytic systems in which the critical reduction step involves a hydride transfer.^{36, 62}
43 Despite being widely present in natural systems, metal-free hydrides lack proper thermodynamic evaluation.
44 Most studies of organic compounds have focused on weaker hydride donors, such as aryl-substituted
45 carbocations and quinones.⁶³⁻⁶⁵ Among stronger organic donors, thermodynamic hydricities have been reported
46 only for a limited number of model compounds.^{56, 63-64, 66-68} The most hydridic donors have found to be radical
47 anions of organic hydride donors, such as one-electron reduced dihydroanthracenes and toluenes.⁶⁸ Even though
48 these radical anionics showed excellent hydride donating ability, very negative potentials required for their
49 formation (< -1.5 V) and low-stability of active hydride species prevent the practical application. As a general
50 trend, the hydricities of these organic hydride donors can be lowered by increasing the stability of the cation R⁺
51 formed upon the hydride transfer, either through aromatic stabilization or by the introduction of electron-
52
53
54
55
56
57
58
59
60

donating groups. Due to experimental challenges associated with determination of ΔG_{H^-} values, the hydricities of metal-free donors are often reported in terms of two other parameters that can be obtained from relatively simple experimental measurements: the enthalpy change associated with the hydride release (ΔH_{H^-})⁶⁹⁻⁷¹ and the hydride nucleophilicity (N).⁷²⁻⁷³ While the reported ΔH_{H^-} values allowed a screening of a large number of metal-free hydrides, it is not clear whether the entropic contribution ($T\Delta S_{H^-}$) is negligible or persistent for structurally different hydride donors. Similarly, the nucleophilicity N is an empirical parameter that provides useful insights into the kinetics of hydride transfers from model donors, but the correlation between N values and standard kinetic parameters (such as activation free energy, ΔG^\ddagger) is not straightforward.



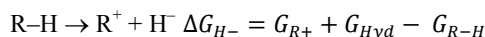
Scheme 1: Structure of organic hydrides: NADH analogs (BNAH, CN-BNAH, Me-MNAH, HEH), methylene tetrahydromethanopterin analogs (BIMH and CAFH), acridine (Ph-AcrH, Me₂N-AcrH, T-AcrH, 4OH, 2OH, 3NH) and triarylmethane (6OH) derivatives.

In this study, we report the calculated and experimental thermodynamic ΔG_{H^-} for model organic hydrides presented in Scheme 1. Some of the model compounds are direct analogs of the enzymatic cofactors NADH¹ (model compounds BNAH, CN-BNAH, Me-MNAH and HEH) and methylene tetrahydromethanopterin H₄MPT⁺⁷⁴ (model compounds BIMH and CAFH). Other model compounds are derived from acridine (Ph-AcrH, Me₂N-AcrH, T-AcrH, 4OH, 2OH, 3NH) and triarylmethane (6OH) frameworks. The calculated values were determined in two solvents using density functional theory (DFT) and supported by experimental findings obtained using electrochemical and hydride transfer methods. A comparison of ΔG_{H^-} values obtained here with calculated ΔH_{H^-} values indicate a degree of uncertainty associated with the evaluation of hydride strength using enthalpic ΔH_{H^-} . In specific, the entropic contribution ($T\Delta S_{H^-}$) was found to differ significantly for structurally unrelated hydride donors. The results of our work were also discussed in terms of the structural and electronic factors that lead to good hydride donor abilities in metal-free models. Importantly, we discovered a new metal-free compound with strong hydride donating ability: an acridine-based structure 3NH was shown to exceed the hydride donor abilities of natural and most artificial metal-free hydride donors. Additionally, the cathodic behavior of the corresponding cation, 3N⁺ was shown to be reversible, indicating that this compound can be utilized in catalysis.

COMPUTATIONAL METHOD

Hydricity calculations. All calculations related to hydricity were performed using Gaussian 09 package⁷⁵ with the resources of the Ohio Supercomputer Center. The geometries of relevant species (R^+ and R-H) were optimized at the ω B97X-D/6-311G(d) level of theory with the conductor-like polarizable continuum model (CPCM) for solvents (acetonitrile and dimethyl sulfoxide).⁷⁶⁻⁷⁸ The frequency calculations were performed to confirm the absence of imaginary frequencies. The output files from the frequency calculations provided the thermal corrections to free energies (ΔG_{corr}^{sol}) for R^+ and R-H. The structures optimized at the ω B97X-D/6-311G(d) level were then used to perform a single-point energy calculation at the ω B97X-D/6-311++G(2df,p)/CPCM(ACN or DMSO) level and the electronic energies (\mathcal{E}_0^{sol}) of R^+ and R-H were obtained from these output files.

The computational method for hydricity calculation was adopted from the previously published study.⁷⁹ The hydricity of a model compound R-H is defined as the thermodynamic driving force (ΔG_{H-}) for the following reaction:



where individual Gibbs free energies are defined as follow:

$$G_{R^+} = (\mathcal{E}_0^{sol} + \Delta G_{corr}^{sol} + \Delta G_{o \rightarrow}^*)_{R^+}$$

$$G_{Hyd} = (\mathcal{E}_0^{gas} + \Delta G_{corr}^{gas} + \Delta G_{hyd}^{sol} + \Delta G_{o \rightarrow}^*)_{Hyd}$$

$$G_{R-H} = (\mathcal{E}_0^{sol} + \Delta G_{corr}^{sol} + \Delta G_{o \rightarrow}^*)_{R-H}$$

where \mathcal{E}_0^{sol} and \mathcal{E}_0^{gas} represent electronic energies in solvated and gas-phases, ΔG_{corr}^{sol} and ΔG_{corr}^{gas} are thermal correction to the Gibbs free energy in solvated and gas-phases, ΔG_{hyd}^{sol} is solvation free energy for the hydride anion and $\Delta G_{o \rightarrow}^*$ is a standard state correction (the value is $\Delta G_{o \rightarrow}^* = +1.891$ kcal/mol for all species that do not have gaseous standard state).⁸⁰⁻⁸¹ Electronic energies and thermal corrections to the Gibbs free energy were obtained as previously described. To derive G_{Hyd} , the electronic energy ($\mathcal{E}_0^{gas} = -331.14$ kcal/mol) and the thermal correction ($\Delta G_{corr}^{gas} = -6.28$ kcal/mol) were obtained for gas-phase using the ω B97X-D/6-31+G(d,p) level of theory. The solvation energy ΔG_{hyd}^{sol} for H^- was obtained from the thermochemical cycle connecting gas phase and solution phase one-electron reduction, as expressed in the following equation:

$$\Delta G_{hyd}^{sol} = \Delta G_{(H/H^-)}^{sol} - \Delta G_{(H/H^-)}^{gas} + \Delta G_{(H)}^{sol}$$

where $\Delta G_{(H/H^-)}^{gas}$ and $\Delta G_{(H/H^-)}^{sol}$ represent the Gibbs free energy changes for the one electron reduction of hydrogen atom in the gas phase and the solution, respectively. $\Delta G_{gas}(H/H^-)$ is the negative value of the electron affinity of hydrogen atom ($\Delta G_{gas}(H/H^-) = -17.39$ kcal/mol⁸²). $\Delta G_{(H/H^-)}^{sol}$ was obtained from the experimental one-electron potentials E_{H/H^-}^0 : using $E_{H/H^-}^0 = -0.60$ V⁶⁸ and -0.55 V⁶⁸ for acetonitrile and dimethyl sulfoxide, $\Delta G_{(H/H^-)}^{sol}$ values were estimated to be -84.88 kcal/mol and -86.04 kcal/mol for acetonitrile and dimethyl sulfoxide, respectively. $\Delta G_{(H)}^{sol}$ represents the solvation energy of hydrogen atom and this value was computed

using CPCM/6-311++G(2df,p) and found to be -0.1 kcal/mol in both solvents. Using this procedure, the computed values for G_{Hyd} were -404.8 kcal/mol and -406.0 kcal/mol for acetonitrile and dimethyl sulfoxide, respectively.

Reduction potential calculations. The first ($E_{R+/R}^0$) and second ($E_{R/R-}^0$) reduction potentials for our model compounds were derived from the calculated driving forces ($\Delta G_{R+/R}$ and $\Delta G_{R/R-}$), as follows:

$$\Delta G_{R+/R} = (\mathcal{E}_0^{sol} + \Delta E_{o\rightarrow}^*)_{R^-} - (\mathcal{E}_0^{sol} + \Delta E_{o\rightarrow}^*)_{R^+}$$

$$\Delta G_{R/R-} = (\mathcal{E}_0^{sol} + \Delta E_{o\rightarrow}^*)_{R^-} - (\mathcal{E}_0^{sol} + \Delta E_{o\rightarrow}^*)_{R}$$

where electronic energies were obtained by performing single-point calculations using the B3LYP⁸³-D3BJ⁸⁴ and ω B97X-D3⁷⁷ exchange correlation functionals with the Def2-TZVP⁸⁵ basis set using the SMD continuum solvation model⁸⁶ on fully optimized structures obtained using the BP86⁸⁷-D3BJ/Def2-SVP⁸⁵ model chemistry with ORCA⁸⁸. The entropic contributions for the reactant and product states were assumed to be similar, which resulted in their mutual cancellation. The ΔG values were then used to calculate the standard reduction potentials ($E = -\frac{\Delta G}{nF}$). The calculated values were referenced to NHE by subtracting 3.92 V⁸⁰ from computed absolute potentials.⁸⁹

In case of second reduction potentials, accuracies of $E_{R/R-}^0$ reduction potentials were systematically improved compared to available experiment when a counter ion (K^+) was included in both the R^- and R^-K^+ states, i.e. using reduction potentials modeled as R^-K^+ and R^-K^+ . It seemed that adding a counter ion stabilizes the anion relative to the neutral radical, and this resulted in better agreement with experiment due to error cancellation. We report our best calculated values in Table 1: first reduction potential was calculated using ω B97X-D3 calculations, while the second reduction potential is calculated with ω B97X-D3 and the counter ion. The Supporting Information (Table S1) reports all calculated data.

EXPERIMENTAL SECTION

General methods. All chemicals were purchased from commercial suppliers and used without further purification. ¹H NMR spectra were recorded on a Bruker Avance III 500 MHz system. Steady-state UV/Vis absorption spectra were recorded on a Varian Cary 50 UV-Vis spectrophotometer. 1-Benzyl-1,4-dihydropyridinamide (BNAH) and 10-Methyl-9-phenylacridinium perchlorate (Ph-Acr⁺) was purchased from TCI America. Fluorene (Flu), triphenylmethane (Ph₃CH), diphenyldiphenylmethane (DPE) and Super-Hydride® (1M in THF) were purchased from Sigma. NAD⁺ analogs (6O⁺,⁹⁰ 4O⁺,⁹⁰ 2O⁺,⁹⁰ 3N⁺,⁹¹ T-Acr⁺,⁹⁰ Me₂N-Acr⁺,⁹⁰ BNA⁺,⁹² CN-BNA⁺,⁹² Me-MNA⁺,⁹³ HE⁺,⁹⁴ BIM⁺,⁹⁵ and CAF⁺,⁹⁶), NADH analogs (6OH,⁹⁷ 2OH,⁹⁸ Ph-AcrH,⁷⁹ CN-BNAH,⁹² BIMH,⁹⁵ CAFH⁹⁶), indicator 9-phenylxanthene (XanH⁹⁹) and nickel-complex ([Ni(dmpe)₂](PF₆)₂)¹⁰⁰) were synthesized according to the previously published procedures.

N,N-dimethyl-4-(10-methyl-9,10-dihydroacridin-9-yl)aniline (Me₂N-AcrH): Me₂N-Acr⁺ (412 mg, 1 mmol) was dissolved in 5 mL ethanol and cooled in an ice bath. Sodium borohydride (150 mg, 4 mmol, 4 eq) was then added and color changed to yellow. The reaction mixture was warmed to room temperature and stirred for

1
2
3 additional 4 hours. Resulting solution was filtered and the precipitate washed with dichloromethane. The filtrate
4 was extracted with dichloromethane, organic extracts were combined and solvent evaporated. The yellow oil was
5 dissolved in ethanol and precipitated by addition of water. The yellow precipitate was filtered, washed with cold
6 water and dried under vacuum to yield 115 g (37%) of pure product. $^1\text{H-NMR}$ (CD_3CN , 500 MHz): 7.30-7.23
7 (4H, m), 7.05 (2H, d), 7.00-6.90 (4H, m), 6.59 (2H, d), 5.13 (1H, s), 3.41 (3H, s), 2.77 (6H, s).
8
9

10
11 **N,N-dimethyl-4-((10-methyl-9,10-dihydroacridin-9-yl)ethynyl)aniline (T-AcrH):** T-Acr $^+$ (120 mg, 0.27
12 mmol) was dissolved in 6 mL ethanol and cooled in an ice bath. Sodium borohydride (62 mg, 1.62 mmol, 6 eq)
13 was added and the reaction mixture was stirred for 2 hours, which resulted in disappearance of deep-blue color.
14 The reaction mixture was then filtered, filtrate disposed and precipitate washed with dichloromethane.
15 Dichloromethane solution was evaporated yielding in 30 mg of brownish product (33%). $^1\text{H-NMR}$ (CD_3CN , 500
16 MHz): 7.67 (2H, d), 7.38 (2H, d), 7.33 (2H, t), 7.10-7.05 (4H, m), 6.73 (2H, d), 5.00 (1H, s), 3.46 (3H, s), 2.98
17 (6H, s).
18
19
20
21

22 **Cyclic voltammetry.** Cyclic voltammetry was performed using a BASi epsilon potentiostat in a VC-2
23 voltammetry cell (Bioanalytical Systems) using platinum working electrode (1.6 mm diameter, MF-2013,
24 Bioanalytical Systems), a nonaqueous Ag/Ag $^+$ reference electrode (MF-2062, Bioanalytical Systems) and a
25 platinum wire (MW-4130, Bioanalytical Systems) as a counter electrode. The spectroscopic grade solvent
26 DMSO and the electrolyte tetrabutylammonium perchlorate (TBAP) were purchased from Sigma Aldrich and
27 used as received. Fast scan rate cyclic voltammetry was performed using CHI 600 C potentiostat and platinum
28 working electrode (CHI-107, CH instruments, 10 μm diameter). In case of T-Acr $^+$, the second standard reduction
29 potential was obtained by oxidation of T-Acr $^-$, which was prepared in-situ from T-AcrH and potassium-
30 dymasil.¹⁰¹ Electrochemical potentials were converted to NHE by adding 0.548 V to the experimental
31 potentials.¹⁰²
32
33
34
35
36

37 **pK_a determination.** The pK_a values of the NADH analogs were determined using the indicator anion method
38 in DMSO.⁹⁹ Under inert atmosphere, indicators (InH) were added to a solution of potassium dymasil
39 ($\text{K}^+\text{CH}_3\text{SOCH}_2^-$) to generate the indicator anions (In $^-$). An excess of indicator solution was added to the
40 $\text{K}^+\text{CH}_3\text{SOCH}_2^-$ to ensure the complete consumption of the base. The anion concentrations were determined
41 using recorded absorbance and In $^-$ extinction coefficients. Then, the colored In $^-$ solutions were quenched by
42 addition of small aliquots of organic hydrides solutions in DMSO. The pK_a values for the organic hydrides were
43 determined using the known indicator pK_a value and experimentally obtained equilibrium constants of the
44 reactions between indicator anions and the hydrides. Indicators were chosen to be within two pK_a units from the
45 hydrides and indicator absorbed in visible spectrum where the other species were transparent.⁹⁹ In case of the
46 overlapping absorptions of In $^-$ and deprotonated hydride R $^-$ ($\text{Me}_2\text{N-Acr}^-$), the absorption of $\text{Me}_2\text{N-Acr}^-$ was
47 subtracted using its extinction coefficient at λ_{max} for indicator In $^-$, as described in Supporting information. The
48 pK_a values of indicators used in this study are:⁹⁹ triphenylmethane (Ph_3CH , pK_a = 30.6) for 4OH,
49 diphenyldiphenylmethane (DPE, pK_a = 29.4) for $\text{Me}_2\text{N-AcrH}$, 9-phenylxanthene (XanH, pK_a = 27.9) for Ph-
50 AcrH and 6OH, fluorene (FIH, pK_a = 22.6) for 2OH.
51
52
53
54
55
56
57
58
59
60

Hydride transfer studies. The hydricities of selected model compounds were obtained by determining the equilibrium constant for the hydride transfer to an appropriate acceptor with known hydride affinity. To ensure that the equilibrium constant can be reached, the reference compounds were selected so that their hydricities are within 3 kcal/mol of the hydricities of our model compounds (as estimated from DFT calculations described in the computational section). The equilibrium concentration ratios of reactants and products were obtained using ^1H NMR spectroscopy. The following steps were performed to ensure that the equilibrium was reached: the progress of the reaction was monitored until the integration of NMR peaks stopped changing. Then, an additional amount of one of the products was added and the reaction was monitored again until the equilibrium was reached. Deuterated acetonitrile and DMSO were used as solvents. All reaction mixtures were prepared in the glove box using dry reagents and air-tight NMR tubes.

Equilibrium of BNAH and 2O^+ : BNAH (3.8 mg, 0.018 mmol) and 2O^+ (8.1 mg, 0.018 mmol) were dissolved in 0.6 mL of deuterated acetonitrile or DMSO. The equilibrium constant was reached after 14 days in acetonitrile yielding $K_{\text{eq}}=9.61$ whereas the equilibrium was reached after 19 days in DMSO yielding $K_{\text{eq}}=1.68$. The hydricity of 2OH in acetonitrile was obtained from K_{eq} and the reported hydricity of BNAH (59 kcal/mol) as reference.⁵⁶ In case of DMSO, the hydricity of 2OH (58.3 kcal/mol) was calculated by using potential-pKa method and the obtained value was used as reference to calculate the hydricity of BNAH in DMSO. The 2OH hydricity was 60 kcal/mol in acetonitrile and the hydricity of BNAH was 57.7 kcal/mol in DMSO.

Equilibrium of BNAH and HE^+ : BNAH (3.8 mg, 0.018 mmol) and HE^+ (5.5 mg, 0.018 mmol) were dissolved in 0.6 mL deuterated acetonitrile or DMSO. In acetonitrile, the equilibrium was reached after 15 days, yielding $K_{\text{eq}}=87.52$. In DMSO, the equilibrium was reached after 49 days, yielding $K_{\text{eq}}=1.53$. The hydricity of HEH in acetonitrile was obtained from K_{eq} and the reported hydricity of BNAH (59 kcal/mol) as reference.⁵⁶ The hydricity of HEH in case of DMSO was obtained from K_{eq} and hydricity of BNAH (57.7 kcal/mol) as reference. The HEH hydricity was 61.5 kcal/mol in acetonitrile and 58.2 kcal/mol in DMSO.

Equilibrium of $[\text{Ni}(\text{dmpe})_2\text{H}]^+$ and 3N^+ or BIM^+ . $[\text{Ni}(\text{dmpe})_2\text{H}]^+$ was prepared in situ by addition of 1M Super-Hydride® (20 μL , 0.020 mmol) to a solution of $[\text{Ni}(\text{dmpe})_2](\text{PF}_6)_2$ (16.2 mg, 0.025 mmol) in 0.6 mL deuterated acetonitrile. To this solution was then added 3N^+ (12.7 mg, 0.025 mmol) or BIM^+ (8.1 mg, 0.026 mmol). The $K_{\text{eq}}=3.33$ was obtained after 15 days for 3N^+ and $K_{\text{eq}}=0.69$ was obtained for BIM^+ after 11 days. From these equilibrium constants and reported hydricity of $[\text{Ni}(\text{dmpe})_2\text{H}]^+$ (49.9 kcal/mol),³⁶ we derived $\Delta G_{\text{H}^-}(3\text{NH})=49.2$ kcal/mol and $\Delta G_{\text{H}^-}(\text{BIMH})=50.1$ kcal/mol in acetonitrile.

RESULTS AND DISCUSSION

Calculated Hydricities. The hydricities ΔG_{H^-} of model compounds R-H (eq 1) are calculated from the absolute Gibbs energies of reactant and product states in the appropriate solvation model:

$$\Delta G_{\text{H}^-} = G_{\text{R}^+} + G_{\text{hyd}} - G_{\text{R-H}} \quad (2)$$

While the Gibbs energies of solvated R^+ and $R-H$ species can be calculated reasonably well using the standard DFT methodology and solvation models, the calculation of absolute Gibbs free energy for the solvated hydride ion (G_{hyd}) represents a challenge. One way to overcome this drawback is to calculate the thermodynamic parameters for a hydride transfer reaction between $R-H$ and a reference hydride acceptor (such as acridinium cation or p-benzoquinone) whose hydride affinity is known from the experiment.^{66, 103} Alternatively, the G_{hyd} value can be obtained as a fitting parameter from the experimental hydricities and calculated Gibbs energies G_{R^+} and G_{R-H} .^{17, 48, 104-105} Unfortunately, G_{hyd} values derived from these studies are not consistent (for example, G_{hyd} values in acetonitrile were reported to be -400.7 kcal/mol,⁴⁸ -404.7 kcal/mol¹⁰⁵ and -412.7 kcal/mol¹⁰⁴).

In collaboration with the Krylov group at the University of Southern California, we previously calculated the hydricity of an acridine-based hydride donor and the obtained value was in excellent agreement with the experimental hydricity.⁷⁹ In our approach, the absolute Gibbs energy G_{hyd} was obtained as the sum of the gas-phase energy G_{hyd}^{gas} and the solvent contribution ΔG_{hyd}^{sol} :

$$G_{hyd} = G_{hyd}^{gas} + \Delta G_{hyd}^{sol} \quad (3)$$

The gas phase energy G_{hyd}^{gas} was calculated using DFT, while the solvation energy ΔG_{hyd}^{sol} was derived from the experimental one-electron reduction potential of hydrogen atom in a solvent of interest⁶⁵ and the calculated gas-phase electron affinity of an H-atom (as detailed in the computational section). The G_{hyd} values obtained in this way are -404.8 kcal/mol (in ACN) and -406.0 kcal/mol (in DMSO). In the current manuscript, this computational methodology was used to calculate the hydricities of our model hydrides in two solvents (ACN and DMSO, Table 1).

Table 1. Calculated standard reduction potentials (vs. NHE) for R^+/R^- and R/R^- , pKa values for RH and $\Delta G_{H\cdot}(RH)$ for RH in different solvents.

Compound	$E_1 (R^+/R^-)^1$	$E_2 (R/R^-)^2$	pKa (RH) ³	$\Delta G_{H\cdot}(RH)^4$	$\Delta G_{H\cdot}(RH)^4$
	DMSO				ACN
6OH	0.08	-1.27	30.4	84.1	85.8
4OH	-0.61	-1.48	37.6	73.2	75.1
PhAcrH	-0.25	-1.17	26.1	72.8	74.9
Me ₂ N-AcrH	-0.30	-1.20	25.6	70.3	72.2
CN-BNAH	-0.69	-1.42	33.1	66.5	68.5
T-AcrH	-0.09	-1.02	14.9	64.7	66.6
2OH	-0.58	-1.40	27.0	61.1	62.9
HEH	-1.04	-1.50	36.0	60.6	62.5
BNAH	-0.94	-1.84	38.4	58.3	60.3
CAFH	-1.87	-1.65	45.8	51.3	53.2
Me-MNAH	-1.24	-1.63	34.1	48.7	50.3
BIMH	-1.51	-1.69	38.4	48.6	50.3
3NH	-1.07	-1.75	30.8	46.9	48.7

¹ Calculated using ω B97X-D3/Def2-TZVP and the SMD continuum solvation model.

² Calculated using ω B97X-D3/Def2-TZVP and the SMD continuum solvation model with a K^+ ion.

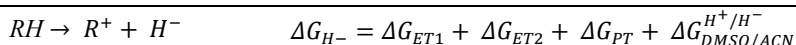
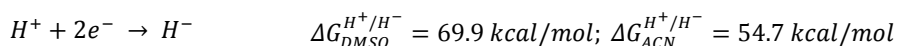
³ Calculated using the equation 4.

⁴ Calculated using ω B97X-D/6-311++G(2df,p)/CPCM (DMSO or ACN).

The calculations were also used to estimate the standard reduction potentials and pKa values of relevant species (Table 1). While $E_1(R^+/R^\cdot)$ values acquired using sole electronic energies showed a reasonable match with experimental values (Table S1, Supporting Information), the $E_2(R^\cdot/R^-)$ values using standard procedures did not match experiment well (mean unsigned error = 0.17 V). Since our original calculated E_2 values were consistently too negative compared to experiment, we speculated this was because the calculated free energies of R^- states were systematically too unstable regardless of different exchange correlation functionals, continuum solvation methods, and basis set sizes. As a simple correction and following previous work,¹⁰⁶ we added a positively charged counter ion, K^+ , into the calculations on the R^- and R^\cdot states, and the resulting E_2 values agreed with available experimental data much better (mean unsigned error = 0.08 V). Adding an analogous counter ion, Cl^- , to the states needed for the E_1 calculations did not improve the agreement of calculated vs. experiment. The obtained calculated reduction potentials are then used to estimate the pKa values for the model hydride donors (eq 4). However, the calculated pKa values (Table 1) are not very accurate. The trends of reduction potentials and pKa values will be discussed in later section when experimental values are introduced.

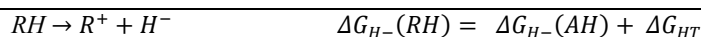
$$pK_a^{RH} = \frac{\Delta G_{H-} - 23.06 (E_{R^+/R^\cdot}^0 + E_{R^\cdot/R^-}^0) - \Delta G_{solvent}^{H^+/H^-}}{1.364} \quad (4)$$

Experimental Hydricities: Two experimental approaches were used to determine the hydricities of model compounds: the “potential-pKa” and “hydride transfer” methods.³⁶ The “potential-pKa method” uses the relevant standard reduction potentials and pKa values to determine the hydricity of a model compound, as follows:



where ΔG_{ET1} and ΔG_{ET2} represent Gibbs free energy changes for first and second electron reduction of NAD^+ analogs, calculated using their reduction potentials (E_{R^+/R^\cdot}^0 and E_{R^\cdot/R^-}^0); ΔG_{PT} represent a Gibbs free energy change for protonation of R^- , calculated using the pKa values of NADH analogs (pK_a^{RH}); $\Delta G_{DMSO}^{H^+/H^-}$ and $\Delta G_{ACN}^{H^+/H^-}$ represent Gibbs free energy changes for two electron reduction of the proton in dimethyl sulfoxide and acetonitrile, respectively, using the derived potentials for proton reduction in these solvents,⁶⁸ ΔG_{H-} represents hydricity of the studied NADH analog.

The “hydride transfer” method involves the determination of the equilibrium constant (K_{HT}) for a hydride transfer from a model hydride R-H and a reference hydride acceptor (A^+) with known affinity, as follows:



where ΔG_{HT} represents a Gibbs free energy change for the hydride transfer between examined and referent hydrides, calculated from experimentally obtained equilibrium constant for the hydride transfer, K_{HT} ; $\Delta G_{H-}(AH)$ and $\Delta G_{H-}(RH)$ represent hydricities of the reference and examined hydrides.

Both of these approaches have limitations, which necessitated the use of “potential-pKa method” for those model compounds that exhibited measurable reduction potentials and pKa values in DMSO. On the other hand, the “hydride transfer” method was used for the model compounds that reached the equilibrium point when reacted with the reference hydride acceptor.

a) Potential-pKa method. While this experimental approach is relatively simple, it is limited to the model compounds whose reduction potentials $E_{R^+/R}^0$ and $E_{R^-/R}^0$ are within the electrochemical window of the electrolyte solution (~ -1.9 V vs. NHE for DMSO using TBAP as electrolyte and platinum working electrode). Furthermore, the pKa values of hydride donors R-H can be experimentally determined only if R-H is more acidic than the solvent (for DMSO, pKa=35, which limits the pKa determination for compounds with pKa values lower than 32).¹⁰⁷ The calculated pKa values in Table 1 indicate that the acidity of CN-BNAH, Me-MNAH, HEH, 4OH, BNAH, BIMH, CAFH are higher than that of the DMSO-limit, indicating that their hydricities are not likely to be determined using the “potential-pKa” method. However, this argument should be taken loosely due to the low accuracy of calculated pKa values. Similarly, the reduction potentials $E_{R^+/R}^0$ and $E_{R^-/R}^0$ need to be less negative than the cathodic electrochemical window of the solvent (~ -1.9 V vs. NHE for DMSO using TBAP as electrolyte and platinum working electrode).

Standard reduction potentials were obtained using cyclic voltammetry (Figure 1). At low sweep rates, the first reduction step of $6O^+$ and most acridine-based models (Ph-Acr⁺, Me₂N-Acr⁺, 4O⁺, 2O⁺ and 3N⁺) exhibited reversible electrochemical behavior, indicating a good chemical stability of the corresponding radicals. On the other hand, the first reduction potentials of pyridinium (CN-BNA⁺, HE⁺, BNA⁺ and Me-MNA⁺) and imidazolium (BIM⁺ and CAF⁺) models appear at more negative potentials and are chemically irreversible, possibly due to radical dimerization.¹⁰⁸⁻¹¹¹ The stability of pyridine-based radicals can be increased by the introduction of substituents in the 4-position.¹¹⁰ The lower reactivity of acridine-based radicals over the pyridine-based structures is likely due to higher delocalization of the unpaired spin in the acridine-based radicals.¹⁰⁹ The reduction of T-Acr⁺ becomes chemically reversible only at high scan rates (2 kV/s, Figure 1), despite the fact that the compound is acridine-based. The origin of the chemical irreversibility has not been explored further, but it is interesting to note that the reduction of the neutral acridine-based analog to form the radical anion is chemically reversible

even at 100 mV/s.¹¹² The chemical instability of imidazolium radicals has been previously attributed to either their dimerization¹¹¹ or to the loss of H-atom and formation of carbene analogs.^{111, 113-115} While the one-electron reduced CAF^+ can form carbene analogs by a loss of a hydrogen atom from the carbon located between two N-centers, it is not clear whether BIM^+ can undergo similar chemistry by a loss of a phenyl radical. The chemical reversibility for the one-electron reduction of pyridinium and imidazolium models could not be achieved (scan rates up to 10 kV/s were investigated), which prevented us from obtaining the standard reduction potentials for these processes.

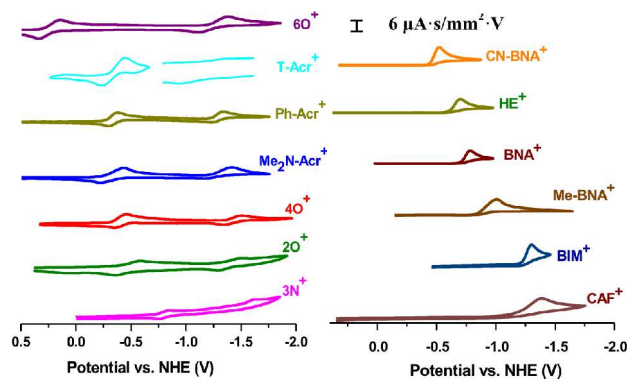


Figure 1. Cyclic voltammograms of model compound (cations) in the cathodic range: Pt working electrode, Pt counter electrode, and nonaqueous Ag/AgNO_3 reference electrode. Sweep rate, 0.1 V/s (3N^+ , CN-BNA^+ , HE^+ , BNA^+ , Me-MBNA^+ , BIM^+ and CAF^+), 25 V/s (6O^+ , T-Acr^+ , $\text{Me}_2\text{N-Acr}^+$, 2O^+), 2 kV/s (T-Acr^+), 100 V/s (Ph-Acr^+ , 4O^+); electrolyte: 0.1 M TBAP in DMSO. The second reduction peak of T-Acr^+ was obtained from the oxidation of T-Acr^- which was formed in situ by the deprotonation of T-AcrH in the presence of dimsyl anion ($\text{pK}_a = 35$).¹⁰⁷

The second reduction peak was obtained only for NAD^+ analogs whose first reduction peaks were reversible (6O^+ , Ph-Acr^+ , $\text{Me}_2\text{N-Acr}^+$, 4O^+ , 2O^+ and 3N^+). At low scan rates (100 mV/s), second reduction peaks were irreversible, likely due to the protonation of the generated anion to form NADH analogs.¹¹⁶ This assignment is consistent with this assignment is the fact that the reactivity of NAD^- anions (reversibility of the second reduction peak) correlates well with pK_a values of the corresponding R-H analogs. For example, the second reduction peak of 6O^+ becomes reversible at relatively low scan rates (25 V/s), which is consistent with relatively low basicity of 6O^- anion (the pK_a of 6OH is 26.9, see text below). On the other hand, the reversibility for 4O^+ requires the scan rates of 100 V/s and the pK_a of 4OH is 30.3 (Table 2). In the case of T-Acr^+ , the standard reduction potential for this process was obtained by electrochemical oxidation of T-Acr^- anion, formed by the deprotonation of T-AcrH (Figure 1). Similar approach was attempted on the compounds that lacked second reduction peaks, but the experiment was not successful because dimsyl-base was not sufficiently strong base to deprotonate hydrides.

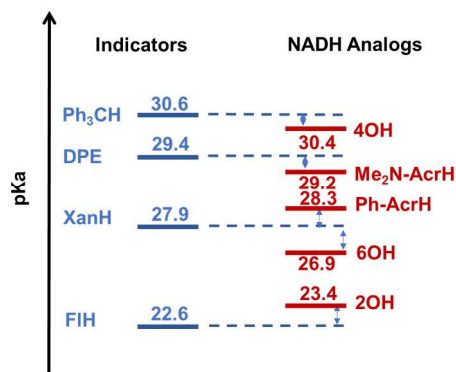


Figure 2. Indicators and their pKa values (left) used to determine the pKa values of NADH analogs (right): triphenylmethane (Ph_3CH), diphenyldiphenylmethane (DPE), 9-phenylxanthene (XanH) and fluorene (FIH).¹⁰⁷

The experimental pKa values for selected hydrides in DMSO were obtained using the spectrophotometric method developed by Bordwell.⁹⁹ The indicators with known pKa values were deprotonated using the dimsyl anion and then reacted with model NADH analogs. The equilibrium constant for the proton transfer between the NADH analog and indicator anion was determined by monitoring the absorption of indicator anion at a selected wavelength (see Figure S2 for example). The accuracy of this method is high (0.05 pKa units) if the acidities of indicator and NADH analog are within 2 pKa units to ensure that the equilibrium is reached.⁹⁹ For this reason, more than one indicator was used to determine the pKa values of model NADH analogs (Figure 2). In case of $\text{Me}_2\text{N-AcrH}$, the absorption of deprotonated NADH analog overlapped with the absorption of indicator anion. In this instance, the absorption contribution due to the deprotonated NADH analog was accounted for, as described in the Supporting Information. Deprotonation of T-AcrH led to unstable products, which prevented us from determining the pKa value of T-AcrH. Also, the same methods could not be applied for the acetonitrile, since the NADH analogs are even weaker acids in this solvent. The obtained pKa values in DMSO were used, along with the standard reduction potentials, to determine the hydricities of model NADH analogs and the values are reported in Table 2.

Table 2. Experimentally obtained $E_{R^+/R}^0$ and $E_{R^-/R}^0$ (V vs. NHE), pK_a^{RH} of NADH model as well as ΔG_{H-} (kcal/mol) values derived using “potential-pKa” method in dimethyl-sulfoxide.

Compound	$E_{R^+/R}^0$	$E_{R^-/R}^0$	pK_a^{RH}	ΔG_{H-}
6OH	+0.24	-1.24	26.9	83.5 ± 3
4OH	-0.38	-1.41	30.4	70.2 ± 3
PhAcrH	-0.29	-1.23	28.3	73.5 ± 2
$\text{Me}_2\text{N-AcrH}$	-0.30	-1.42	29.2	70.1 ± 2
T-AcrH	-0.22	-1.07	N/A	N/A
2OH	-0.50	-1.39	23.4	58.2 ± 2
3NH	-0.80	-1.62	N/A	N/A

b) Hydride Transfer Method. The hydricities of almost one half of the model NADH analogs presented in Scheme 1 could not be obtained using the potential-pKa method (either due to the irreversible reduction behavior of NAD⁺ analogs or due to the high pKa values of the corresponding R-H). The hydricities of these model compounds were obtained using the hydride-transfer method, which was previously used by Dubois to obtain the hydricities of NADH-analogs (BNAH and CN-BNAH) in acetonitrile, using the metal-based hydride donors as references.⁵⁶ This study showed that the accurate equilibrium constants can be obtained if the hydricities of two relevant hydrides differ by less than 3 kcal/mol. In our study, NMR spectroscopy was used to determine the hydricities of model NADH analogs in two solvents: acetonitrile and dimethyl sulfoxide, and the results are listed in Table 3. As an example, the NMR spectra for the reaction between BNAH (reference hydride) and 2O⁺ in acetonitrile is presented in Figure S3, Supporting Information. Unfortunately, the hydride transfer method could not be applied to all model compounds, due to the occurrence of unwanted side reactions. Experimental hydricity values obtained potential-pKa and hydride transfer methods are further validated by cross-referencing among studied model compounds (see Supporting Information for more details).

Table 3. Hydricities (ΔG_{H^-} , kcal/mol) of selected model NADH analogs obtained using “hydride-transfer” method in dimethylsulfoxide and acetonitrile.

	Compound	Reference Hydride (ΔG_{H^-})	ΔG_{H^-}
DMSO	BNAH	2OH (58.2)	57.5 ± 2
	HEH	BNAH (57.5)	58 ± 2
		2OH (58.2)	57.9 ± 2
ACN	BNAH	CpRe(NO)(CO)(CHO) ¹ (55)	$59^1 \pm 2$
	2OH	BNAH (59) ¹	60.3 ± 2
	HEH	BNAH (59) ¹	61.5 ± 2
		CNBNAH (63) ¹	61 ± 2
	CN-BNAH	BNAH (59) ¹	$63^1 \pm 2$
	BIMH	[Ni(dmpe) ₂ H] ⁺ (49.9) ³⁶	50.1 ± 2
	3NH	[Ni(dmpe) ₂ H] ⁺ (49.9) ³⁶	49.2 ± 2

¹Ref. ⁵⁶

Theory vs. Experiment. The experimental hydricities obtained using “potential-pKa” and “hydride transfer” methods showed a good match with the calculated values (Figure 3). The calculated values are frequently higher than the experimental hydricities by up to 3 kcal/mol, likely due in part to the uncertainties associated with the treatment of the hydride ion solvation in calculations. A similar match between experiment and theory has been reported previously for metal-based hydrides.^{33, 48} Our finding that computationally-inexpensive methods reproduce the experimental hydricities is quite encouraging, particularly in light of technical difficulties associated with determination of experimental values.

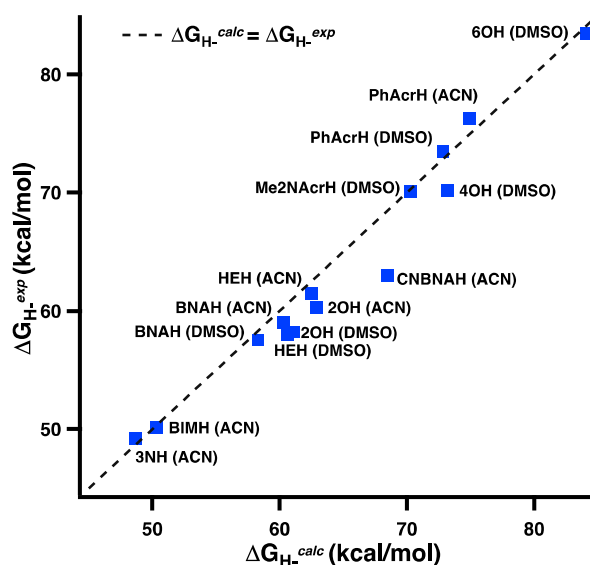


Figure 3. Comparison between the calculated and experimental hydricities for the NADH-analogs. The value for PhAcrH was obtained from our ref.⁷⁹, while the values for BNAH and CN-BNAH were obtained from ref.⁵⁶

Entropic contributions. The experimental determination of ΔG_{H^-} values can be quite challenging, as shown in the previous section. On the other hand, the enthalpy for hydride transfer ΔH_{H^-} is readily obtained by a simple calorimetry method, and this method has been used to screen a large number of metal-free hydride donors. While the enthalpy approach is quite useful, the use of ΔH_{H^-} to describe hydride donor ability is justified only when entropic contributions are negligible. To evaluate the entropic contribution, we compared the ΔG_{H^-} and ΔH_{H^-} values obtained by us and others^{56, 69, 71, 103, 117-119} in Figure 4. The data clearly show that the entropic contribution for metal-free hydrides cannot be ignored, with $T\Delta S_{H^-}$ -values ranging from 3.4 to 12.1 kcal/mol. Thus, the assumption that the entropic contribution can be neglected introduces, on average, a 10% error to the measurement.

A more accurate approach is to assume that the entropic contribution is constant across a series of structurally related hydride donors. This assumption was found to be valid for tungsten hydride complexes ($T\Delta S_{H^-} = 3.2$ kcal/mol).⁵⁴ While this assumption drastically reduces the error, the ΔS_{H^-} values are not always constant across series. NADH analogs exhibit $T\Delta S_{H^-}$ values in a narrow range (4.4 – 5.2 kcal/mol), whereas the acridine derivatives were found to have values in much wider range (3.4 – 6.5 kcal/mol). Thus, the enthalpic hydricity ΔH_{H^-} can be used to predict trends within the structurally related hydride donors, but it fails to give precise driving forces for hydride transfer reactions with hydrides of different groups.

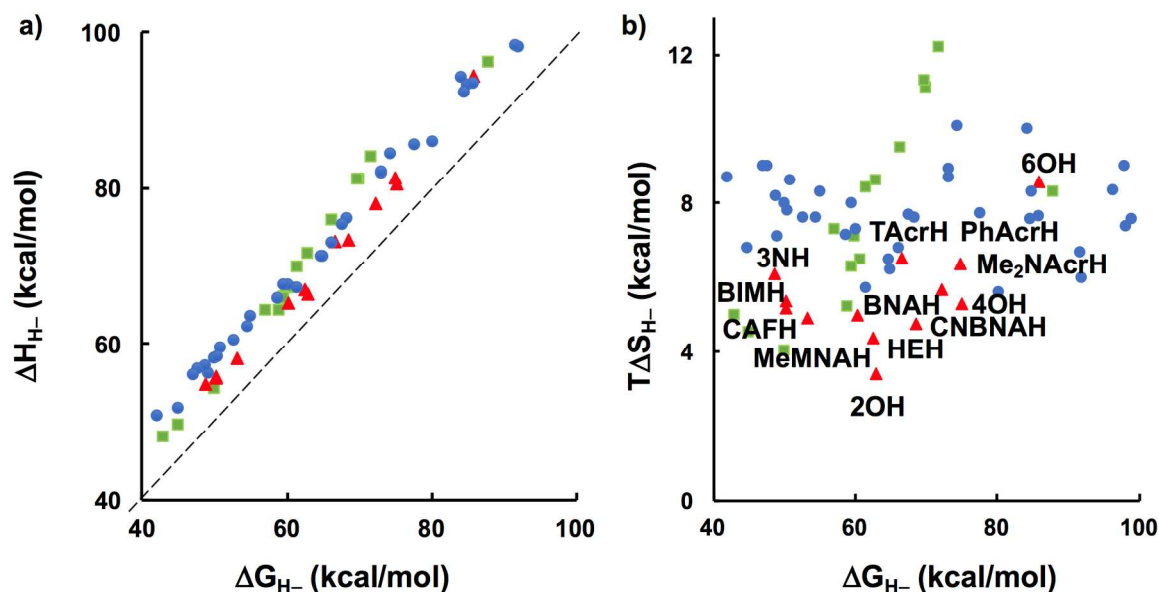


Figure 4. a) Comparison between ΔH_{H^-} and ΔG_{H^-} for organic and other metal-free hydride donors in acetonitrile. b) Comparison between $T\Delta S_{H^-}$ and ΔG_{H^-} for organic hydride donors. Hydrides are represented as follows: calculated values for hydrides studied here (red triangles), calculated values by others (blue circles) and experimental values obtained elsewhere (green squares).

Structure-Property Relationship. Based on the calculated and experimental data presented here, several interesting points can be raised regarding the structural factors that control hydricities of organic donors. In general, the hydride donor ability of R-H derivatives improves with an increase in the stabilization of the forming cation, R^+ . Consequently, triarylmethane derivative showed the poorest hydride donor ability, where the R^+ stabilization is achieved solely through nonaromatic delocalization. The positive charge in R^+ can be stabilized through the inductive effect of electron-donating substituents, as can be observed for the NADH-analogs, where the replacement of electron-withdrawing amide (BNAH, $\Delta G_{H^-} = 59$ kcal/mol) or cyano (CN-BNAH, $\Delta G_{H^-} = 63$ kcal/mol) groups with the electron-donating methyl group (Me-MNAH, $\Delta G_{H^-} = 50$ kcal/mol) has a strong effect on hydricity. In another example, the hydricity of Me₂N-AcH ($\Delta G_{H^-} = 70.1$ kcal/mol) is lower relative to the derivative without donating group (PhAcH, $\Delta G_{H^-} = 73.5$ kcal/mol).

An interesting class of hydride donors are imidazoles (BIMH and CAFH), which have shown low hydricities (calculated ACN values in the 50-53 kcal/mol range) in accordance from previously reported ΔH_{H^-} .⁶⁹ The high hydride donor ability of imidazole derivatives has been previously credited to the specific conformation and an anomeric effect,¹²⁰ where neighboring nitrogen centers destabilize the C-H bond in R-H by donating their lone pairs to its antibonding orbital. It is interesting to note that imidazole-based hydride donors have been identified in a relatively new class of hydrogenases, namely 5,10-methenyltetrahydromethanopterin (Hmd) hydrogenase.¹²¹ In this enzyme, the imidazole-based hydride donor drives H₂-heterolysis reaction, activated by the presence of Fe-containing cofactor. Since the synthetic procedures for these derivatives are relatively straightforward, it is likely that new imidazole-based hydride donors will be reported in the near future.

1
2
3
4 Strikingly, the strongest hydride donor among the studied compounds was found to be an acridine derivative,
5 3NH (calculated $\Delta G_{H^-} = 49$ kcal/mol in ACN). This finding is surprising, considering that the increase in the
6 number of fused aromatic rings leads to the lowering of aromatic stabilization in the corresponding R^+ cation. For
7 example, dihydro-pyridines are better hydride donors than dihydro-acridines, because of the higher aromatic
8 character of pyridinium cation.¹⁰³ In the case of $3N^+$, the aromatic moiety is stabilized through the positive charge
9 delocalization via the conjugation with the remainder of the molecule. In addition, a significant structural strain
10 present in the rigid 3NH further facilitates the loss of a hydride ion, resulting in a highly planar system. The
11 effects of extended charge delocalization and planarization prevails in $4OH < 2OH < 3NH$ series where hydricity
12 in ACN declines from 75 kcal/mol to 49 kcal/mol.
13
14
15
16
17

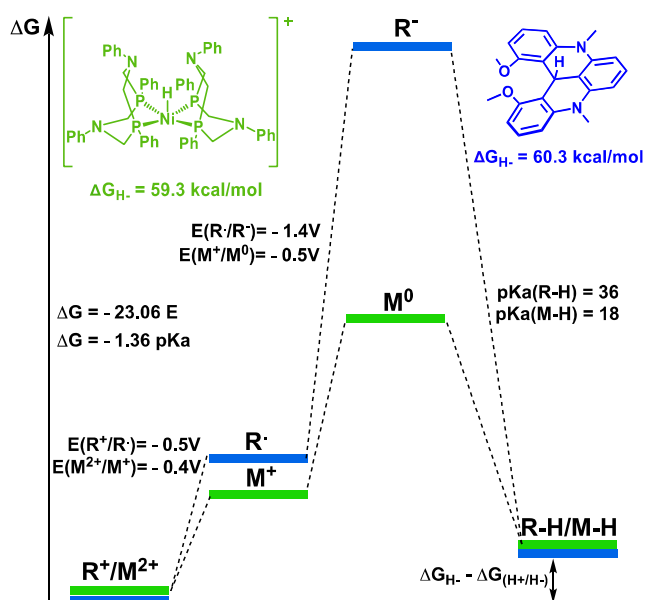
18 It is interesting to note that acridine-based hydrides studied here (3NH and 2OH) have comparable hydricity
19 values to other known reducing reagent, such as sodium borohydride ($NaBH_4$, calculated $\Delta G_{H^-} = 50$ kcal/mol¹¹⁷
20 in ACN) and Hantzsch ester ($\Delta G_{H^-} = 59$ kcal/mol¹¹⁷ in ACN). Despite being commonly utilized in organic
21 synthesis, these hydrides are used in stoichiometric rather catalytic amounts, due to challenges associated with
22 their regeneration.¹²² The electrochemical recovery of NADH-analogs is complicated by the chemical side
23 reactions involving one-electron reduced species (such as radical dimerization).¹⁰⁸⁻¹⁰⁹ Unlike NADH-analogs,
24 $3N^+$ and $2O^+$ exhibit electrochemically and chemically reversible reduction potentials (Figure 1), suggesting that
25 3NH and 2OH can be electrochemically recovered and could possibly serve as renewable hydride donors.
26
27
28
29

30 Overall, the hydride donor abilities were improved slightly going from acetonitrile to dimethyl sulfoxide (by ~
31 2 kcal/mol), which was also predicted by calculations. Such a trend can be explained by the small differences in
32 their dielectric constants ($\epsilon(\text{DMSO}) = 47$ vs. $\epsilon(\text{ACN}) = 38$), which results in slightly better solvation of formed
33 charged species (R^+ and H^-). A similar solvent trend has been observed for the Ni-based hydride,⁴⁰ whose
34 hydricities were obtained in acetonitrile ($\Delta G_{H^-} = 57.4$ kcal/mol), dimethyl sulfoxide ($\Delta G_{H^-} = 55.5$ kcal/mol) and
35 water ($\Delta G_{H^-} = 30.0$ kcal/mol).
36
37
38
39

40 **Comparison with metal-based analogs.** Transition metal hydrides have been identified as important
41 intermediates in a variety of catalytic fuel-forming and other redox reactions in ground and excited state.^{35, 45, 123-}
42 ¹²⁷ On the other hand, the metal-free hydrides have not been widely used for this purpose, despite the abundance
43 of enzymatic catalysis by NADH, $FADH_2$ and other metal-free hydrides.^{1-5, 121} Thus, it is interesting to compare
44 the thermodynamic hydricities of our model compounds with those reported for metal-based hydrides. In general,
45 the hydricities of metal-based hydrides span a wide range of values (reported acetonitrile hydricities are in the
46 26-120 kcal/mol range^{34, 36}). The metal-free hydrides of Scheme 1 exhibit values that are somewhat higher, with
47 the calculated values in the 49-86 kcal/mol range, and seem to have hydricities similar to the first row transition
48 metal hydrides, such as Co, Ni and Fe-based compounds (acetonitrile hydricities are in the 32-73 kcal/mol
49 range³⁶). Thus, both types of compounds are sufficiently strong hydride donors for the relevant fuel forming
50
51
52
53
54
55
56
57
58
59
60

1
2
3 reactions. For example, the hydride affinity of protons in acetonitrile is ~ -76.6 kcal/mol,⁴³ indicating that most
4 metal-free hydride donors in Scheme 1 are thermodynamically capable of driving the hydrogen evolution
5 reaction.
6
7
8
9

10 Why are then metal-free hydride donors not used in fuel-forming reactions as often as their metal-based
11 analogs? One possible explanation might be related to the differences in the activation barriers associated with
12 the relevant hydride transfer processes (our future studies will investigate the kinetic effect in more detail).
13 Another reason for lower use of metal-free hydride catalysts might be related to the closure of catalytic cycle,
14 which involves the two-electron, proton-coupled reduction of R^+ to recover the active R-H hydride form. To
15 exemplify this point, Figure 5 presents an energy diagram for two hydride donors of similar hydricities: a metal-
16 based $[\text{Ni}(\text{P}^{\text{Ph}}_2\text{N}^{\text{Ph}})_2\text{H}]^+$ complex, whose hydricity in acetonitrile is $\Delta G_{\text{H}^-} = 59.3$ kcal/mol,¹²⁸ and 2OH, whose
17 hydricity is $\Delta G_{\text{H}^-} = 60.3$ kcal/mol. The first reduction potentials of the corresponding precursors, $E(\text{M}^{2+}/\text{M}^+)$ and
18 $E(\text{R}^+/\text{R}^\cdot)$, are relatively similar and affordably small (around -0.5 V vs. NHE). Previous studies of metal-based
19 compounds have shown that $E(\text{M}^{2+}/\text{M}^+)$ shifts to more negative values as the hydride donor ability of the
20 corresponding donor increases.^{36, 52, 129-131} Our metal-free analogs scale in the same way, as exemplified by the
21 similarities in the first reduction peaks for M^{2+}/M^+ and $\text{R}^+/\text{R}^\cdot$. However, a striking difference was observed in the
22 values for the second reduction potentials, $E(\text{M}^+/\text{M}^0)$ and $E(\text{R}^\cdot/\text{R}^-)$: while the metal-based compound undergoes
23 the second reduction at a relatively low potential (-0.5 V vs. NHE), the metal-free model compound requires a
24 significantly more negative potential (-1.4 V vs. NHE) to inject the second electron.
25
26
27
28
29
30
31
32
33
34
35
36
37



1
2
3 **Figure 5.** The comparison of energy diagram profiles for the regeneration of active hydride forms of metal-
4 based ($[\text{Ni}(\text{P}^{\text{Ph}}_2\text{N}^{\text{Ph}})_2\text{H}]^+$)¹²⁸ and metal-free (2OH) hydride donors.
5
6
7

8
9
10
11
12
13
14
15
16
17
18
19
20
21
22
23
24
25
26
27
28
29
30
31
32
33
34
35
36
37
38
39
40
41
42
43
44
45
46
47
48
49
50
51
52
53
54
55
56
57
58
59
60
Such a large energy requirement for the second reduction step prohibits the application of metal-free hydride donors in catalysis. Several approaches can be used to lower the standard reduction potentials in metal-free systems. One involves the coupling of the first electron transfer step with a proton transfer to generate RH^+ , which will then be reduced at a less negative potential. Such proton-coupled reduction has been selected by nature as a way to regenerate NADH. Specifically, NAD^+ reduction is mediated by FADH_2 , which is formed from FAD^+ through two proton-coupled reductions.¹³² Another interesting approach towards the lowering of reduction potentials has recently been reported by Berben and coworkers, who utilized the coordination with Al ions to lower the reduction potentials of imine-based ligands.³² Finally, model compounds that exhibit small or even inverted differences in reduction potentials can be utilized to facilitate the regeneration of metal-free hydrides.¹³³ For example, it was shown for some organic compounds that the structural changes that accompany the first electron reduction can result in the lowering of their LUMO orbital energies and associated second reduction potentials.¹³⁴ We observe similar effects in the case of BIM^+ , which exhibits the smallest energy difference between the calculated $E(\text{R}^+/\text{R}\cdot)$ and $E(\text{R}\cdot/\text{R}^-)$ potentials (Table 1), likely brought about by the rotation of the phenyl ring upon one electron reduction (Figure S4, Supporting Information).

CONCLUSIONS

Despite their importance in enzymatic redox reactions, metal-free hydride donors are not widely used as catalysts for fuel-forming and other reduction processes. To explore their applicability in catalysis, we investigated hydricities of several model compounds that are direct analogs of the enzymatic cofactors NADH and methylene tetrahydromethanopterin, as well as the synthetic hydrides derived from acridine and triarylmethane frameworks. The hydride donor ability for the model compounds reported here were found to be similar to metal-based hydrides and dependent on structural motifs, such as size of conjugated molecular framework, aromaticity and presence of electron-donating groups. Unlike the metal-based equivalents, the metal-free hydrides exhibited high values for their second reduction potentials, prohibiting the catalyst recovery. Future design of these hydride donors will be focused on the lowering the reduction potentials and enabling the facile hydride-form regeneration.

SUPPORTING INFORMATION

The Supporting Information is available free of charge on the [ACS Publications website](#) at

¹H NMR spectra, coordinates for optimized structures, calculated reduction potentials, pKa-determination experiment and hydride-transfer method, enthalpic contributions.

AUTHOR INFORMATION

Corresponding Author

* glusac@uic.edu

ORCID

Ksenija D. Glusac: 0000-0002-2734-057X

John A. Keith: 0000-0002-6583-6322

Stefan Ilic: 0000-0002-6305-4001

ACKNOWLEDGEMENTS

K.D.G. thanks ACS PRF (54436-ND4) for financial support and Ohio Supercomputer Center (PCS0201-5) for computational support. J.A.K. acknowledges support from the R.K. Mellon Foundation, ACS PRF (55595-DNI4) and the National Science Foundation (CBET-1653392).

Reference

1. Hummel, W., *Trends Biotechnol.* **1999**, *17* (12), 487-492.
2. Reda, T.; Plugge, C. M.; Abram, N. J.; Hirst, J., *Proc. Natl. Acad. Sci. U.S.A.* **2008**, *105* (31), 10654-10658.
3. Schrittwieser, J. H.; Velikogne, S.; Kroutil, W., *Adv. Synth. Catal.* **2015**, *357* (8), 1655-1685.
4. Stueckler, C.; Hall, M.; Ehammer, H.; Pointner, E.; Kroutil, W.; Macheroux, P.; Faber, K., *Org. Lett.* **2007**, *9* (26), 5409-5411.
5. Stuermer, R.; Hauer, B.; Hall, M.; Faber, K., *Curr. Opin. Chem. Biol.* **2007**, *11* (2), 203-213.
6. Rueping, M.; Sugiono, E.; Azap, C.; Theissmann, T.; Bolte, M., *Org. Lett.* **2005**, *7* (17), 3781-3783.
7. Ouellet, S. G.; Walji, A. M.; Macmillan, D. W., *Acc. Chem. Res.* **2007**, *40* (12), 1327-1339.
8. Zheng, C.; You, S.-L., *Chem. Soc. Rev.* **2012**, *41* (6), 2498-2518.
9. Rueping, M.; Antonchick, A. P.; Theissmann, T., *Angew. Chem. Int. Ed.* **2006**, *45* (22), 3683-3686.
10. Yang, J. W.; List, B., *Org. Lett.* **2006**, *8* (24), 5653-5655.
11. Yang, J. W.; Hechavarria Fonseca, M. T.; List, B., *Angew. Chem. Int. Ed.* **2004**, *43* (48), 6660-6662.
12. Ouellet, S. G.; Tuttle, J. B.; MacMillan, D. W., *J. Am. Chem. Soc.* **2005**, *127* (1), 32-33.
13. Seshadri, G.; Lin, C.; Bocarsly, A. B., *J. Electroanal. Chem.* **1994**, *372* (1), 145-150.

14. Barton, E. E.; Rampulla, D. M.; Bocarsly, A. B., *J. Am. Chem. Soc.* **2008**, *130* (20), 6342-6344.
15. Polyansky, D.; Cabelli, D.; Muckerman, J. T.; Fujita, E.; Koizumi, T. a.; Fukushima, T.; Wada, T.; Tanaka, K., *Angew. Chem. Int. Ed.* **2007**, *46* (22), 4169-4172.
16. Costentin, C.; Canales, J. C.; Haddou, B.; Savéant, J.-M., *J. Am. Chem. Soc.* **2013**, *135* (47), 17671-17674.
17. Lim, C.-H.; Holder, A. M.; Hynes, J. T.; Musgrave, C. B., *J. Am. Chem. Soc.* **2014**, *136* (45), 16081-16095.
18. Lim, C.-H.; Holder, A. M.; Hynes, J. T.; Musgrave, C. B., *J. Phys. Chem. Lett.* **2015**, *6* (24), 5078-5092.
19. Keith, J. A.; Carter, E. A., *Chem. Sci.* **2013**, *4* (4), 1490-1496.
20. Keith, J. A.; Carter, E. A., *J. Phys. Chem. Lett.* **2013**, *4* (23), 4058-4063.
21. Lessio, M.; Senftle, T. P.; Carter, E. A., *ACS Energy Lett.* **2016**, *1* (2), 464-468.
22. Liao, K.; Askerka, M.; Zeitler, E. L.; Bocarsly, A. B.; Batista, V. S., *Top. Catal.* **2015**, *58* (1), 23-29.
23. Bocarsly, A. B.; Gibson, Q. D.; Morris, A. J.; L'Esperance, R. P.; Detweiler, Z. M.; Lakkaraju, P. S.; Zeitler, E. L.; Shaw, T. W., *ACS Catalysis* **2012**, *2* (8), 1684-1692.
24. Portenkirchner, E.; Enengl, C.; Enengl, S.; Hinterberger, G.; Schlager, S.; Apaydin, D.; Neugebauer, H.; Knör, G.; Sariciftci, N. S., *ChemElectroChem* **2014**, *1* (9), 1543-1548.
25. Lee, J. H.; Lauw, S. J.; Webster, R. D., *Electrochem commun.* **2016**, *64*, 69-73.
26. Xiang, D.; Magana, D.; Dyer, R. B., *J. Am. Chem. Soc.* **2014**, *136* (40), 14007-14010.
27. Saveant, J.-M.; Tard, C. d., *J. Am. Chem. Soc.* **2016**, *138* (3), 1017-1021.
28. Lim, C.-H.; Holder, A. M.; Hynes, J. T.; Musgrave, C. B., *J. Phys. Chem. B* **2017**, *121* (16), 4158-4167.
29. Giesbrecht, P. K.; Herbert, D. E., *ACS Energy Lett.* **2017**, *2* (3), 549-555.
30. Kobayashi, K.; Ohtsu, H.; Nozaki, K.; Kitagawa, S.; Tanaka, K., *Inorg Chem* **2016**, *55* (5), 2076-2084.
31. Sato, S.; Morikawa, T., *ChemPhotoChem* **2017**, Published Online: October 6, 2017 doi: 10.1002/cptc.201700133.
32. Thompson, E. J.; Berben, L. A., *Angew. Chem. Int. Ed.* **2015**, *54* (40), 11642-11646.
33. Qi, X.-J.; Fu, Y.; Liu, L.; Guo, Q.-X., *Organometallics* **2007**, *26* (17), 4197-4203.
34. DuBois, D. L., *Inorg Chem* **2014**, *53* (8), 3935-3960.
35. Bullock, R. M.; Appel, A. M.; Helm, M. L., *Chem. Comm.* **2014**, *50* (24), 3125-3143.
36. Wiedner, E. S.; Chambers, M. B.; Pitman, C. L.; Bullock, R. M.; Miller, A. J.; Appel, A. M., *Chem. Rev.* **2016**, *116* (15), 8655-8692.
37. Pitman, C. L.; Brereton, K. R.; Miller, A. J., *J. Am. Chem. Soc.* **2016**, *138* (7), 2252-2260.
38. Brereton, K. R.; Bellows, S. M.; Fallah, H.; Lopez, A. A.; Adams, R. M.; Miller, A. J.; Jones, W. D.; Cundari, T. R., *J. Phys. Chem. B* **2016**, *120* (50), 12911-12919.
39. Garg, K.; Matsubara, Y.; Ertem, M. Z.; Lewandowska-Andralojc, A.; Sato, S.; Szalda, D. J.; Muckerman, J. T.; Fujita, E., *Angew. Chem. Int. Ed.* **2015**, *54* (47), 14128-14132.

- 1
2
3
4
5
6
7
8
9
10
11
12
13
14
15
16
17
18
19
20
21
22
23
24
25
26
27
28
29
30
31
32
33
34
35
36
37
38
39
40
41
42
43
44
45
46
47
48
49
50
51
52
53
54
55
56
57
58
59
60
40. Tsay, C.; Livesay, B. N.; Ruelas, S.; Yang, J. Y., *J. Am. Chem. Soc.* **2015**, *137* (44), 14114-14121.
 41. Taheri, A.; Berben, L. A., *Inorg Chem* **2015**, *55* (2), 378–385.
 42. Creutz, C.; Chou, M. H., *J. Am. Chem. Soc.* **2007**, *129* (33), 10108-10109.
 43. Wayner, D. D.; Parker, V. D., *Acc. Chem. Res.* **1993**, *26* (5), 287-294.
 44. Curtis, C. J.; Miedaner, A.; Ellis, W. W.; DuBois, D. L., *J. Am. Chem. Soc.* **2002**, *124* (9), 1918-1925.
 45. DuBois, D. L.; Berning, D. E., *Appl. Organomet. Chem.* **2000**, *14* (12), 860-862.
 46. Labinger, J. A.; Komadina, K. H., *J. Organomet. Chem.* **1978**, *155* (2), C25-C28.
 47. Curtis, C. J.; Miedaner, A.; Raebiger, J. W.; DuBois, D. L., *Organometallics* **2004**, *23* (3), 511-516.
 48. Nimlos, M. R.; Chang, C. H.; Curtis, C. J.; Miedaner, A.; Pilath, H. M.; DuBois, D. L., *Organometallics* **2008**, *27* (12), 2715-2722.
 49. Miedaner, A.; Haltiwanger, R. C.; DuBois, D. L., *Inorg Chem* **1991**, *30* (3), 417-427.
 50. Raebiger, J. W.; Miedaner, A.; Curtis, C. J.; Miller, S. M.; Anderson, O. P.; DuBois, D. L., *J. Am. Chem. Soc.* **2004**, *126* (17), 5502-5514.
 51. Berning, D. E.; Noll, B. C.; DuBois, D. L., *J. Am. Chem. Soc.* **1999**, *121* (49), 11432-11447.
 52. Berning, D. E.; Miedaner, A.; Curtis, C. J.; Noll, B. C.; Rakowski DuBois, M. C.; DuBois, D. L., *Organometallics* **2001**, *20* (9), 1832-1839.
 53. Wilson, A. D.; Miller, A. J.; DuBois, D. L.; Labinger, J. A.; Bercaw, J. E., *Inorg Chem* **2010**, *49* (8), 3918-3926.
 54. Ellis, W. W.; Ciancanelli, R.; Miller, S. M.; Raebiger, J. W.; Rakowski DuBois, M.; DuBois, D. L., *J. Am. Chem. Soc.* **2003**, *125* (40), 12230-12236.
 55. Roberts, J. A.; Appel, A. M.; DuBois, D. L.; Bullock, R. M., *J. Am. Chem. Soc.* **2011**, *133* (37), 14604-14613.
 56. Ellis, W. W.; Raebiger, J. W.; Curtis, C. J.; Bruno, J. W.; DuBois, D. L., *J. Am. Chem. Soc.* **2004**, *126* (9), 2738-2743.
 57. Ceballos, B. M.; Tsay, C.; Yang, J. Y., *Chem. Comm.* **2017**, *53* (53), 7405-7408
 58. Creutz, C.; Chou, M. H., *J. Am. Chem. Soc.* **2009**, *131* (8), 2794-2795.
 59. Connelly, S. J.; Wiedner, E. S.; Appel, A. M., *Dalton Trans.* **2015**, *44* (13), 5933-5938.
 60. Taheri, A.; Thompson, E. J.; Fettinger, J. C.; Berben, L. A., *ACS Catalysis* **2015**, *5* (12), 7140-7151.
 61. Robinson, S. J. C.; Zall, C. M.; Miller, D. L.; Linehan, J. C.; Appel, A. M., *Dalton Trans.* **2016**, *45* (24), 10017-10023.
 62. Waldie, K. M.; Ostericher, A. L.; Reineke, M.; Sasayama, A. F.; Kubiak, C. P., *ACS Catalysis* **2017**.
 63. Cheng, J.; Handoo, K. L.; Parker, V. D., *J. Am. Chem. Soc.* **1993**, *115* (7), 2655-2660.
 64. Cheng, J.; Handoo, K. L.; Xue, J.; Parker, V. D., *J. Org. Chem.* **1993**, *58* (19), 5050-5054.
 65. Parker, V., *Acta Chem. Scand.* **1992**, *46* (11), 1133-1134.
 66. Zhu, X.-Q.; Wang, C.-H.; Liang, H.; Cheng, J.-P., *J. Org. Chem.* **2007**, *72* (3), 945-956.

- 1
2
3
4
5
6
7
8
9
10
11
12
13
14
15
16
17
18
19
20
21
22
23
24
25
26
27
28
29
30
31
32
33
34
35
36
37
38
39
40
41
42
43
44
45
46
47
48
49
50
51
52
53
54
55
56
57
58
59
60
67. Zhang, X.-M.; Bruno, J. W.; Enyinnaya, E., *J. Org. Chem.* **1998**, *63* (14), 4671-4678.
68. Handoo, K. L.; Cheng, J. P.; Parker, V. D., *J. Am. Chem. Soc.* **1993**, *115* (12), 5067-5072.
69. Zhu, X.-Q.; Zhang, M.-T.; Yu, A.; Wang, C.-H.; Cheng, J.-P., *J. Am. Chem. Soc.* **2008**, *130* (8), 2501-2516.
70. Han, X.; Hao, W.; Zhu, X.-Q.; Parker, V. D., *J. Org. Chem.* **2012**, *77* (15), 6520-6529.
71. Zhu, X.-Q.; Tan, Y.; Cao, C.-T., *J. Phys. Chem. B* **2010**, *114* (5), 2058-2075.
72. Richter, D.; Tan, Y.; Antipova, A.; Zhu, X. Q.; Mayr, H., *Chem. Asian J.* **2009**, *4* (12), 1824-1829.
73. Richter, D.; Mayr, H., *Angew. Chem. Int. Ed.* **2009**, *48* (11), 1958-1961.
74. Hiromoto, T.; Warkentin, E.; Moll, J.; Ermler, U.; Shima, S., *Angew. Chem. Int. Ed.* **2009**, *48* (35), 6457-6460.
75. Frisch, M. J.; Trucks, G. W.; Schlegel, H. B.; Scuseria, G. E.; Robb, M. A.; Cheeseman, J. R.; Scalmani, G.; Barone, V.; Mennucci, B.; Petersson, G. A.; Nakatsuji, H.; Caricato, M.; Li, X.; Hratchian, H. P.; Izmaylov, A. F.; Bloino, J.; Zheng, G.; Sonnenberg, J. L.; Hada, M.; Ehara, M.; Toyota, K.; Fukuda, R.; Hasegawa, J.; Ishida, M.; Nakajima, T.; Honda, Y.; Kitao, O.; Nakai, H.; Vreven, T.; Montgomery Jr., J. A.; Peralta, J. E.; Ogliaro, F.; Bearpark, M. J.; Heyd, J.; Brothers, E. N.; Kudin, K. N.; Staroverov, V. N.; Kobayashi, R.; Normand, J.; Raghavachari, K.; Rendell, A. P.; Burant, J. C.; Iyengar, S. S.; Tomasi, J.; Cossi, M.; Rega, N.; Millam, N. J.; Klene, M.; Knox, J. E.; Cross, J. B.; Bakken, V.; Adamo, C.; Jaramillo, J.; Gomperts, R.; Stratmann, R. E.; Yazyev, O.; Austin, A. J.; Cammi, R.; Pomelli, C.; Ochterski, J. W.; Martin, R. L.; Morokuma, K.; Zakrzewski, V. G.; Voth, G. A.; Salvador, P.; Dannenberg, J. J.; Dapprich, S.; Daniels, A. D.; Farkas, Ö.; Foresman, J. B.; Ortiz, J. V.; Cioslowski, J.; Fox, D. J. *Gaussian 09*, Gaussian, Inc.: Wallingford, CT, USA, 2009.
76. Chai, J.-D.; Head-Gordon, M., *J. Chem. Phys.* **2008**, *128* (8), 084106.
77. Chai, J.-D.; Head-Gordon, M., *Phys. Chem. Chem. Phys.* **2008**, *10* (44), 6615-6620.
78. Barone, V.; Cossi, M., *J. Phys. Chem. A* **1998**, *102* (11), 1995-2001.
79. Yang, X.; Walpita, J.; Zhou, D.; Luk, H. L.; Vyas, S.; Khnayzer, R. S.; Tiwari, S. C.; Diri, K.; Hadad, C. M.; Castellano, F. N., *J. Phys. Chem. B* **2013**, *117* (49), 15290-15296.
80. Kelly, C. P.; Cramer, C. J.; Truhlar, D. G., *J. Phys. Chem. B* **2007**, *111* (2), 408-422.
81. Muckerman, J. T.; Skone, J. H.; Ning, M.; Wasada-Tsutsui, Y., *Biochim. Biophys. Acta* **2013**, *1827* (8), 882-891.
82. Lykke, K.; Murray, K.; Lineberger, W., *Phys. Rev. A* **1991**, *43* (11), 6104.
83. Becke, A. D., *J. Chem. Phys.* **1993**, *98* (7), 5648-5652.
84. Grimme, S.; Ehrlich, S.; Goerigk, L., *J. Comput. Chem.* **2011**, *32* (7), 1456-1465.
85. Weigend, F.; Ahlrichs, R., *Phys. Chem. Chem. Phys.* **2005**, *7* (18), 3297-3305.
86. Marenich, A. V.; Cramer, C. J.; Truhlar, D. G., *J. Phys. Chem. B* **2009**, *113* (18), 6378-6396.
87. Perdew, J. P., *Phys. Rev. B* **1986**, *33* (12), 8822.
88. Neese, F., *Wiley Interdiscip Rev Comput Mol Sci* **2012**, *2* (1), 73-78.

- 1
2
3 89. Isse, A. A.; Gennaro, A., *J. Phys. Chem. B* **2010**, *114* (23), 7894-7899.
- 4 90. Ilic, S.; Brown, E. S.; Xie, Y.; Maldonado, S.; Glusac, K. D., *J. Phys. Chem. C*
5 **2016**, *120* (6), 3145-3155.
- 6 91. W Laursen, B.; C Krebs, F., *Chem. Eur. J.* **2001**, *7* (8), 1773-1783.
- 7 92. Paul, C. E.; Gargiulo, S.; Opperman, D. J.; Lavandera, I.; Gotor-Fernández, V.;
8 Gotor, V.; Taglieber, A.; Arends, I. W.; Hollmann, F., *Org. Lett.* **2012**, *15* (1), 180-183.
- 9 93. Huang, S.; Wong, J. C.; Leung, A. K.; Chan, Y. M.; Wong, L.; Fernandez, M. R.;
10 Miller, A. K.; Wu, W., *Tetrahedron Lett.* **2009**, *50* (35), 5018-5020.
- 11 94. Ogata, Y.; Takagi, K.; Tanabe, Y., *Perkin Trans.* **1979**, (8), 1069-1071.
- 12 95. Lee, C. K.; Lee, I.-S. H., *Heterocycles* **2009**, *78* (2), 425-433.
- 13 96. Hori, M.; Kataoka, T.; Shimizu, H.; Imai, E.; Matsumoto, Y., *Chem. Pharm. Bull.*
14 **1985**, *33* (9), 3681-3688.
- 15 97. Carey, F. A.; Tremper, H. S., *J. Am. Chem. Soc.* **1968**, *90*, 2578-2583.
- 16 98. Guin, J.; Besnard, C.; Pattison, P.; Lacour, J., *Chem. Sci.* **2011**, *2* (3), 425-428.
- 17 99. Matthews, W. S.; Bares, J. E.; Bartmess, J. E.; Bordwell, F.; Cornforth, F. J.;
18 Drucker, G. E.; Margolin, Z.; McCallum, R. J.; McCollum, G. J.; Vanier, N. R., *J. Am.*
19 *Chem. Soc.* **1975**, *97* (24), 7006-7014.
- 20 100. Robinson, S. J. C.; Zall, C. M.; Miller, D. L.; Linehan, J. C.; Appel, A. M., *Dalton*
21 *Trans.* **2016**, *45* (24), 10017-10023.
- 22 101. Cheng, J.-P.; Lu, Y.; Zhu, X.; Mu, L., *J. Org. Chem.* **1998**, *63* (18), 6108-6114.
- 23 102. Pavlishchuk, V. V.; Addison, A. W., *Inorg. Chim. Acta.* **2000**, *298* (1), 97-102.
- 24 103. Shi, J.; Huang, X.-Y.; Wang, H.-J.; Fu, Y., *J. Chem. Inf. Model.* **2011**, *52* (1), 63-
25 75.
- 26 104. Muckerman, J. T.; Achord, P.; Creutz, C.; Polyansky, D. E.; Fujita, E., *Proc. Natl.*
27 *Acad. Sci. U.S.A.* **2012**, *109* (39), 15657-15662.
- 28 105. Kovács, G.; Pápai, I., *Organometallics* **2006**, *25* (4), 820-825.
- 29 106. Keith, J. A.; Grice, K. A.; Kubiak, C. P.; Carter, E. A., *J. Am. Chem. Soc.* **2013**,
30 *135* (42), 15823-15829.
- 31 107. Bordwell, F. G., *Acc. Chem. Res.* **1988**, *21* (12), 456-463.
- 32 108. Hapiot, P.; Moiroux, J.; Saveant, J. M., *J. Am. Chem. Soc.* **1990**, *112* (4), 1337-
33 1343.
- 34 109. Anne, A.; Hapiot, P.; Moiroux, J.; Savéant, J.-M., *J. Electroanal. Chem.* **1992**,
35 *331* (1-2), 959-970.
- 36 110. Hermolin, J.; Levin, M.; Kosower, E. M., *J. Am. Chem. Soc.* **1981**, *103* (16),
37 4808-4813.
- 38 111. de Robillard, G.; Devillers, C. H.; Kunz, D.; Cattey, H.; Digard, E.; Andrieu, J.,
39 *Org. Lett.* **2013**, *15* (17), 4410-4413.
- 40 112. Elangovan, A.; Chiu, H.-H.; Yang, S.-W.; Ho, T.-I., *Org. Biomol. Chem.* **2004**, *2*
41 (21), 3113-3118.
- 42 113. Gorodetsky, B.; Ramnial, T.; Branda, N. R.; Clyburne, J. A., *Chem. Comm.* **2004**,
43 (17), 1972-1973.
- 44 114. Ogawa, K. A.; Boydston, A. J., *Chem. Lett.* **2014**, *43* (6), 907-909.
- 45 115. Han, X.; Hao, W.; Zhu, X.-Q.; Parker, V. D., *The Journal of organic chemistry*
46 **2012**, *77* (15), 6520-6529.
- 47 116. Koper, N.; Jonker, S.; Verhoeven, J.; Van Dijk, C., *Recl. Trav. Chim. Pays-Bas*
48 **1985**, *104* (11), 296-302.
- 49
50
51
52
53
54
55
56
57
58
59
60

- 1
2
3 117. Heiden, Z. M.; Lathem, A. P., *Organometallics* **2015**, *34* (10), 1818-1827.
4 118. Matsubara, Y.; Fujita, E.; Doherty, M. D.; Muckerman, J. T.; Creutz, C., *J. Am.*
5 *Chem. Soc.* **2012**, *134* (38), 15743-15757.
6 119. Kreevoy, M. M.; Ostovic, D.; Lee, I. S. H.; Binder, D. A.; King, G. W., *J. Am.*
7 *Chem. Soc.* **1988**, *110* (2), 524-530.
8 120. Brunet, P.; Wuest, J. D., *J. Org. Chem.* **1996**, *61* (6), 2020-2026.
9 121. Shima, S.; Pilak, O.; Vogt, S.; Schick, M.; Stagni, M. S.; Meyer-Klaucke, W.;
10 Warkentin, E.; Thauer, R. K.; Ermler, U., *Science* **2008**, *321* (5888), 572-575.
11 122. McSkimming, A.; Colbran, S. B., *Chem. Soc. Rev.* **2013**, *42* (12), 5439-5488.
12 123. Rakowski Dubois, M.; Dubois, D. L., *Acc. Chem. Res.* **2009**, *42* (12), 1974-1982.
13 124. Thoi, V. S.; Sun, Y.; Long, J. R.; Chang, C. J., *Chem. Soc. Rev.* **2013**, *42* (6),
14 2388-2400.
15 125. Miller, A. J.; Labinger, J. A.; Bercaw, J. E., *Organometallics* **2011**, *30* (16), 4308-
16 4314.
17 126. Pitman, C.; Finster, O.; Miller, A., *Chem. Comm.* **2016**, *52* (58), 9105-9108.
18 127. Barrett, S. M.; Pitman, C. L.; Walden, A. G.; Miller, A. J., *J. Am. Chem. Soc.*
19 **2014**, *136* (42), 14718-14721.
20 128. Frazee, K.; Wilson, A. D.; Appel, A. M.; Rakowski DuBois, M.; DuBois, D. L.,
21 *Organometallics* **2007**, *26* (16), 3918-3924.
22 129. Yang, J. Y.; Bullock, R. M.; Shaw, W. J.; Twamley, B.; Frazee, K.; DuBois, M. R.;
23 DuBois, D. L., *J. Am. Chem. Soc.* **2009**, *131* (16), 5935-5945.
24 130. Galan, B. R.; Schöffel, J.; Linehan, J. C.; Seu, C.; Appel, A. M.; Roberts, J. A.;
25 Helm, M. L.; Kilgore, U. J.; Yang, J. Y.; DuBois, D. L., *J. Am. Chem. Soc.* **2011**, *133*
26 (32), 12767-12779.
27 131. Yang, J. Y.; Smith, S. E.; Liu, T.; Dougherty, W. G.; Hoffert, W. A.; Kassel, W.
28 S.; DuBois, M. R.; DuBois, D. L.; Bullock, R. M., *J. Am. Chem. Soc.* **2013**, *135* (26),
29 9700-9712.
30 132. Carrillo, N.; Ceccarelli, E. A., *Eur. J. Biochem.* **2003**, *270* (9), 1900-1915.
31 133. Evans, D. H., *Chem. Rev.* **2008**, *108* (7), 2113-2144.
32 134. Evans, D. H.; Busch, R. W., *J. Am. Chem. Soc.* **1982**, *104* (19), 5057-5062.
33
34
35
36
37
38
39
40

